Effects of d-electrons in pseudopotential screened-exchange density functional calculations

Byounghak Lee and Lin-Wang Wang

Computational Research Division, Lawrence Berkeley National Laboratory, Berkeley, California 94720

Andrew Canning

Computational Research Division, Lawrence Berkeley National Laboratory, Berkeley, California 94720 and Department of Applied Science, University of California, Davis, California 95616

Abstract

We report a theoretical study on the role of shallow d states in the screened-exchange local density approximation (sX-LDA) band structure of binary semiconductor systems. We found that inaccurate pseudo-wavefunctions can lead to 1) an overestimation of the screened-exchange interaction between the localized d states and the delocalized higher energy s and p states and 2) an underestimation of the screened-exchange interaction between the d states. The resulting sX-LDA band structures have substantially smaller band gaps compared with experiments. We correct the pseudo-wavefunctions of d states by including the semicore s and p states of the same shell in the valence states. The correction of pseudo-wavefunctions yields band gaps and d state binding energies in good agreement with experiments and the full potential linearized augmented plane wave sX-LDA calculations. Compared with the quasi-particle GW method, our sX-LDA results shows not only similar quality on the band gaps but also much better d state binding energies. Combined with its capability of ground state structure calculation, the sX-LDA is expected to be a valuable theoretical tool for the II-VI and III-V (especially the III-N) bulk semiconductors and nanostructure studies.

PACS numbers: 71.15.Mb, 71.20.Nr

I. INTRODUCTION

The vast majority of modern *ab initio* condensed matter calculations are based on the density functional theory (DFT). [1] The Kohn-Sham (KS) scheme[2] made it possible to apply the DFT to realistic systems by mapping the many-body systems to auxiliary single particle systems, and has been proven to be extremely successful for the ground state properties. Among different numerical methods to solve the KS equations, pseudopotential (PP) methods are particularly favored due to their computational efficiency resulting from the replacement of the sharp ionic potential with a much softer one.[3–5] The remarkable success of the PP method relies on the fact that the core states, i.e., the states whose atomic eigenvalues are much lower than the valence states, are inert to the changes in the electron density outside of the so called core-radius. The norm-conservation condition on the PP's guarantees that the net electron density in PP calculations inside the core-radius agrees with the electron density in all-electron (AE) calculations and, at the same time, the wavefunctions outside of the core-radius are the same in PP and AE methods.

The screened-exchange local density approximation (sX-LDA) method was proposed as an example of the generalized Kohn-Sham (GKS) scheme to overcome the well-known *band gap problem* in KS schemes.[6, 7] While still within the auxiliary non-interacting electron scheme, GKS includes the energy functional which has an explicit wavefunction dependence. It has been demonstrated that the sX-LDA within the plane wave pseudopotential method is very successful for many of group III-V and IV semiconductors.[7] Preliminary calculations on group II-VI and some of group III-V semiconductors, however, show that the sX-LDA method with local density approximation (LDA) norm conserving PP's yields poor band gaps. The common features of these semiconductors is the presence of shallow cation d states. In contrast, it has been reported that the sX-LDA without PP's within the full-potential linearized augmented plane wave (FLAPW) method is accurate regardless of the presence of shallow d states.[8] In this paper, we discuss the role of the shallow d states in the sX-LDA method.

Our major findings are as follow. 1) In the presence of shallow d states, the sX-LDA with the conventional LDA pseudopotentials predicts band gaps substantially smaller than experiments. This is due to the pseudo-wavefunction error in the LDA pseudopotentials. 2) The pseudopotential sX-LDA band gap can be corrected by including the semicore s and

p states. This procedure improves the nonlocal screened-exchange interaction by forcing the valence pseudowavefunctions to agree with all-electron (AE) wavefunctions outside of a very short radius. 3) The inclusion of semi-core states also improves the d state position in sX-LDA. While the sX-LDA band gap is comparable to the GW band gap, the d state position in sX-LDA is actually in much better agreement with experiments.

II. METHOD

The single particle states in the sX-LDA method are found by minimizing the total energy defined as

$$E_{\rm tot}[v] = T + E_{\rm H}[\rho] + E_{\rm sX}[\{\psi\}] + R[\rho] + E_{\rm ext}[v] \tag{1}$$

with the electron density defined as

$$\rho(\mathbf{r}) = \sum_{i}^{occ} |\psi_i(\mathbf{r})|^2. \tag{2}$$

In Eq.(1), T, $E_{\rm H}[\rho]$, and $E_{\rm ext}[v]$ are the kinetic energy, the direct Hartree Coulomb energy, and the external potential energy, respectively. The screened-exchange energy is defined with a Thomas-Fermi screening function;

$$E_{\rm sX}[\{\psi\}] = -\frac{1}{2}\sum_{i,j}^{\rm occ}\int\int d\mathbf{r}d\mathbf{r}'\frac{\psi_i^*(\mathbf{r})\psi_j^*(\mathbf{r}')\psi_j(\mathbf{r})\psi_i(\mathbf{r}')e^{-k_{TF}|\mathbf{r}-\mathbf{r}'|}}{|\mathbf{r}-\mathbf{r}'|}, \tag{3}$$

where k_{TF} is the screening length determined from the average density of electrons. Note that this screened-exchange term eliminates the spurious self-interaction in LDA at short range, where the error is larger. The band gap correction in sX-LDA in most semiconductors is in part due to the corrected self-interaction.[9–12] $R[\rho]$ is the difference between the LDA exchange-correlation energy and the local approximation of the screened-exchange energy, $E_{\rm sX}[\{\psi\}]$;

$$R[\rho] = E_{\rm xc}^{\rm LDA}[\rho] - E_{\rm sX}^{\rm loc}[\rho]\ , \tag{4}$$

where

$$E_{\rm sX}^{\rm loc}[\rho] = \int d\mathbf{r}\rho(\mathbf{r})\ \epsilon_{\rm x}^{\rm LDA}[\rho]\ F\left[\frac{k_{TF}}{k_F}\right]\ , \tag{5}$$

$$\epsilon_{\rm x}^{\rm LDA}[\rho] = -\frac{3}{4}\left(\frac{3}{\pi}\right)^{1/3}\rho^{1/3}\ , \tag{6}$$

$$F[x] = 1 - \frac{4}{3}x \arctan\left(\frac{2}{x}\right) - \frac{x^2}{6}\left\{1 - \left(\frac{x^2}{4} + 3\right)\ln\left(1 + \frac{4}{x^2}\right)\right\}. \quad (7)$$

Here $\epsilon_{\rm x}^{\rm LDA}[\rho]$ is the LDA exchange energy density and k_F is the Fermi wavevector. Following the suggestion of Ref. 6 and 7, we use the average charge density for k_F. The resulting Kohn-Sham equation is

$$(-\frac{1}{2}\nabla^2 + V_H + V_{\rm xc}^{\rm LDA} - V_{\rm sX}^{\rm loc}(\mathbf{r}) + V_{\rm ext})\psi_i(\mathbf{r}) + \int d\mathbf{r}' V_{\rm sX}(\mathbf{r},\mathbf{r}')\psi_i(\mathbf{r}') = \epsilon_i\psi_i(\mathbf{r}) \ , \quad (8)$$

where $V_{\rm sX}$ is the non-local screened-exchange operator,

$$V_{\rm sX}(\mathbf{r},\mathbf{r}') = -\sum_i^{\rm occ} \frac{\psi_i(\mathbf{r})e^{-k_{TF}|\mathbf{r}-\mathbf{r}'|}\psi_i^*(\mathbf{r}')}{|\mathbf{r}-\mathbf{r}'|} \ . \quad (9)$$

Note that PP's are usually derived from the LDA formalism and, as a result, they do not guarantee the adequacy in the nonlocal sX-LDA formalism. Strictly speaking, this way of constructing PP's is not consistent with the sX-LDA approach. A better way is to construct a PP within the sX-LDA formalism so that PP sX-LDA results agree with the AE sX-LDA results. It is known from the exact exchange (EXX) method that PP's generated within EXX can be substantially different from the ones generated within LDA.[13] It has also been shown that the optimal screening length of the sX-LDA method in the atomic configurations is very different from the bulk Thomas-Fermi screening length.[14] However, because of the nonlocality of the sX-LDA formalism, just as in Harree-Fock theory[15] and EXX method[16], there is no rigorous way to generate the sX-LDA pseudopotentials. To our knowledge, all the previous plane wave sX-LDA studies have used PP's generated within the LDA method. This situation is rather analogous to that of GW calculations, where the LDA PP's are used without any modification. This is the topic of the current paper. Previous studies indicate that the LDA PP's work well for sX-LDA when d states are not present.[7] Therefore, we believe it is a practical approach to apply the LDA PP's to the sX-LDA formalism and to understand any problem in the LDA-PP sX-LDA calculations, and to correct these problems based on our understanding.

The question regarding the LDA PP's in sX-LDA arises from the orbital dependence of $E_{\rm sX}[\{\psi\}]$. The difference between the AE wavefunctions and the pseudo-wavefunction in the core region causes errors in the screened-exchange integral of Eq(3), which have not been taken into account in the PP generation based on LDA formalism. To investigate the effects of PP in the presence of shallow d-states, we follow the procedure prescribed in GW

studies by Rohlfing *et al.*[17] and Luo *et al.*.[18] Two sets of cation atom PP's are studied; 1) (+12/+13) PP's with d electrons and the outer shell electrons in the valence. The numbers in the parenthesis denotes the number of valence electrons used in the PP calculation for column II and III cations respectively. 2) (+20/+21) PP's with entire semicore s, p, and d electrons as well as the outer shell electrons in the valence. For example, in case of Zn atom, (+12) Zn PP includes $3d$ and $4s$ electrons in the valence. (+20) Zn PP, on the other hand, includes $3s$, $3p$, $3d$, and $4s$ electrons in the valence. For lower charge state cation atoms, *i.e.* $(+12/+13)$ PP, we use the conventional norm conserving PP's. For higher charge state cation atoms, *i.e.* $(+20/+21)$ PP, we first construct the PP for an ion without the outer shell electrons and then vary the core-radius of each PP angular momentum channel to fit the eigenvalues of the neutral atom configuration. For instance, for a Zn atom we first build a (Ne)$3s^2 3p^6 3d^{10}$ PP. This (+20) Zn PP is used for (Ne)$3s^2 3p^6 3d^{10} 4s^2$ configuration, and the eigenvalues are compared with the AE calculation results. This complicated procedure is required because, in conventional pseudopotential generators, only one reference state for one angular momentum can be used. Our PP's yield good outer shell eigenvalues with the energy discrepancy < 0.1 eV and the d state eigenvalues with the energy discrepancy $\lesssim 0.15$ eV. This is shown in Table I. Although there is a small difference in the d state energy, we found that this does not cause any significant change in the band gap in the following calculations. In calculations presented here, we did not include core-charge corrections in either of the pseudopotentials, (+12/+13) PPs or (+20/+21) PPs. This correction might be important for total energy calculations but we found it is not crucial in eigen energies,

The inclusion of semicore states is computationally demanding because highly localized semicore states require a large plane wave cutoff energy. We determined the cutoff energies so that the energy eigenvalues in LDA calculations converged to within 1 meV. The cutoff energies used for (+20/+21) PP [(+12/+13) PP] are 200 [60] , 250 [80], 200 [80], 200 [80] Ry for ZnSe, ZnS, CdS, InN, respectively. The increased number of orbitals in non-local screened-exchange potential in Eq.(9) also contributes to a larger computational cost. In general, sX-LDA calculations with semicore electrons are approximately 10 times more expensive than sX-LDA calculations with only valence electrons.

III. RESULTS AND DISCUSSIONS

The effects of inclusion of semicore states on the valence pseudo-wavefunctions are shown in Fig. 1. The most notable difference between (+12) Zn PP wavefunctions and (+20) Zn PP is the overall location of the d orbitals. The center of mass of the all electron d orbital and that of (+20) Zn PP is much closer to the nucleus than the d orbital of (+12) Zn PP. This results in the much smaller overlap between the d states and the delocalized s and p states. In addition, the nodal structure of the valence wavefunctions are changed thanks to the orthonormality condition with the semicore states.

The error introduced by the usage of the pseudopotentials can be analyzed in terms of the screened-exchange integral between the atomic orbitals. The screened-exchange interaction between the atomic orbitals $\{\phi_\alpha\}$ is

$$K_{\alpha\beta\gamma\delta} = \int d\mathbf{r}_1 \int d\mathbf{r}_2 \phi^*_\alpha(\mathbf{r}_1)\phi^*_\beta(\mathbf{r}_2)\phi_\gamma(\mathbf{r}_1)\phi_\delta(\mathbf{r}_2)\frac{e^{-k_{TF}|\mathbf{r}_1-\mathbf{r}_2|}}{|\mathbf{r}_1-\mathbf{r}_2|}, \tag{10}$$

where α, β, γ, and δ are the composite quantum numbers consisting of the orbital angular momenta, l and m, and the spin, σ. Note that the opposite spins do not contribute to the exchange integral. As for the screening length, k_{TF}, we have chosen a typical bulk screening length using the average valence charge density, including s and p states. In Table I we show the screened-exchange integral $K_{l,l'} \equiv K_{l,l',l',l}$ of neutral atomic configurations. For the sake of simplicity, we averaged the integral over the magnetic quantum number, m, and restricted ourselves to the integral of the two orbitals l and l'. The screened-exchange integral between the highest s and p states, i.e., K_{ss}, K_{pp}, and K_{sp}, are almost identical to AE results regardless of the PP's. This is because the s and p wavefunctions have nodes at similar radius and, as a result, they have little weight in the nodal points. Therefore, the nodal structure of these wavefunctions is of less importance in the exchange integral between themselves. In the case of d orbitals, however, the nodal structure and the center of mass positions of the wavefunctions play an important role in the determining the screened-exchange integral. The larger overlap between the d orbitals and the s and p orbitals of (+12/+13) PP is reflected in the large $K_{sd}(+12/+13)/K_{sd}(AE)$ and $K_{pd}(+12/+13)/K_{pd}(AE)$. The larger error of $K_{sd}(+20/+21)$ and $K_{pd}(+20/+21)$ relative to $K_{dd}(+20/+21)$ probably stems from the nodal structure error in the s and p pseudo-wavefunctions. The screened-exchange integral is smaller for wider spread wavefunctions because of the $e^{-k_{TF}r}/r$ screened Coulomb

interaction. d-d overlap, therefore, is much smaller in (+12/+13) PP calculations than in (+20+21) PP and the AE calculations.

We point out that the ionic pseudopotentials are not intended to replace the neutral atom pseudopotentials. Our purpose in introducing the ionic pseudopotential is to address the problem with d states in the sX-LDA method. Constructed to fit AE valence electron eigenenergies, ionic (+20/+21) PPs lose some of the tranferability of norm-conserving pseudopotentials and, consequently, yield results that are slightly different from their (+12/+13) PP counterparts. As shown in Table II, the LDA band gap of (+20/+21) PPs is smaller than the LDA band gap of (+12/+13) PPs by ≈ 0.05 eV. The position of d states appears to suffer more from the lack of transferability; the calculated LDA results for d states position with (+20/+21) PPs are consistently shallower than the results with (+12/+13) PPs by 0.3 - 0.5 eV. As we shall show below, the main effects of the screened-exchange interaction is to increase the band gap and to deepen the d states energy. Should the LDA trend persist, the (+20/+21) PP sX-LDA results with more accurate pseudopotentials will increase the band gap and deepen the d state energy even further, making the method closer to experiments.

Having established the fact that the full semicore states are necessary for proper d orbitals in sX-LDA, we calculate the electronic structure of test systems where the shallow d states are essential. Fig. 2 shows the band structure of ZnS calculated with (+12) Zn PP and (+20) Zn PP. For (+12) Zn PP, the top valence bands are almost identical in LDA and sX-LDA (after a rigid shift for valence band maximum alignment). The notable changes in sX-LDA are the band gap increase as well as the deepening of d band position and the lower Zn s bands. Although improved by ~ 0.7 eV over LDA, the sX-LDA band gap, 2.41 eV, is too small compared with experimental value of 3.78 eV when (+12) Zn PP is used. The inclusion of the whole Zn semicore states, as shown in Fig. 2 (b), further increase the gap between the valence bands and the conduction bands by ~ 0.8 eV, and makes the comparison with experiment much better. The relative position of d bands, however, undergoes a relatively small change,~ 0.2 eV.

The changes of band structure can be further analyzed by looking at the absolute eigenvalues of the KS equations. Fig. 3 shows the band edge states of ZnS. The energies are plotted relative to the LDA valence band maximum (VBM) energy for each PP. The absolute eigenvalues in sX-LDA are generally down-shifted compared with LDA eigenvalues. This is because the screened-exchange potential is always negative. The sX-LDA band

gaps are larger than those of LDA because the valence bands are pulled down even more than the conduction bands. The comparison between the sX-LDA results with different PP's shows that the inclusion of the semicore s and p states makes the conduction band down-shift smaller, while keeping the valence bands and the d states almost unchanged, relative to LDA results. In other words, the error in d state wavefunctions in (+12) Zn PP causes the overestimation of the conduction band-d states exchange interaction and leads to a underestimation of the band gap.

In addition to ZnS, we studied effects of d states in the sX-LDA for ZnSe, CdS, and InN. The results are summaries in Table II. For all the systems studied, the sX-LDA with (+12/+13) PP's, i.e., PP's without semicore s and p states, yield substantially smaller band gaps compared with experiments. When the full semicore states are included in PP's, the sX-LDA band gaps are improved and the results are comparable to GW results. The band gap discrepancy between the sX-LDA results and the experiments is $\lesssim 0.5$ eV in all cases. The d electron binding energies (the energy differences between the VBM and the d states) are improved from LDA, but improvement over (+12/+13) PPs varies. This is because of the difference in the correction of the screened-exchange interaction. An increase of the exchange interaction with d states deepens the d state energy. In the case of Cd and In, the change (+12/+13) PP $\rightarrow$ (+20/+21) PP increases the $d-d$ interaction by a small amount ($5 \sim 20\%$) but decreases $s-d$ and $p-d$ interactions by as much as $60 \sim 80\%$. The overall d state energies in CdS and InN become shallower in (+20/+21) PPs calculations. To the contrary, for Zn atom, the increase in the $d-d$ interaction by (+12/+13) PP $\rightarrow$ (+20/+21) PP is large, 40%. As a result, the d state energies in ZnSe and ZnS decreases. The d electron binding energy discrepancy is within 0.5 eV of experimental values. In comparison, the GW d electron binding energy has a larger error than sX-LDA.

We have also compared our plane wave semicore PP sX-LDA results with AE sX-LDA results. The reported FLAPW sX-LDA band gaps from Ref. [8] are shown in Table II. The band gap difference between the PP and FLAPW sX-LDA are 0.31, 0.15, and 0.43 eV for CdS, ZnSe, and ZnS, respectively. These differences are similar in amplitudes to the differences between the semicore PP and FLAPW LDA results. Because of our approximated way of generating the semicore PP, the LDA discrepancy between the semicore PP and FLAPW is slightly larger than difference between the conventional PP and FLAPW. Nevertheless, we believe the general good agreement between the semicore PP and FLAPW sX-LDA results

confirms the correctness of both methods.

Finally, we discuss an alternate approach to address the effects of d states. Without introducing the semicore s and p states, the over-extended semicore d states can be corrected by a small core radius in the conventional PP method. We tested this approach by using a Zn PP with a core radius $r_c^{3d} = 1.0$ Bohr in a ZnS calculation. Table. III shows the comparison among different PP methods. When a Zn^{+12} PP with short core radius is used, the $d-d$ screened-exchange integral, K_{dd}, improves similarly to the Zn^{+20} PP but K_{sd} and K_{pd} are still rather poor compared to the Zn^{+20} PP results due to the lack of nodal structure. The larger K_{sd} and K_{pd} result in overestimation of the $3d$ states position. Computation-wise, this approach has no advantage as the energy needed for plane wave convergence is comparable to that of Zn^{+20} PP.

IV. SUMMARY

We have investigated the effects of d electrons in the plane wave pseudopotential screened-exchange LDA calculations. The inclusion of the cation d electrons is important in many II-VI and III-V semiconductors as their energies are close to the valence s and p levels. However, we found that, when the conventional norm conserving LDA PP is used, the sX-LDA band gaps become much smaller than the experimental results. We have identified the problem: the pseudo wavefunctions deviate considerably from the all electron wavefunctions, in particular for their center of mass positions. Although these pseudo wavefunctions can reproduce the AE LDA results, they cannot represent the screened-exchange integrals of the AE wavefunctions. We have thus generated PP's with semicores. With the inclusion of the semicores, the pseudo wavefunctions become similar to the AE wavefunctions, and the amplitudes of the screened-exchange integrals have been restored. The same problem exists in plane wave pseudopotential GW calculations, and similar semicore PP's have been used in previous GW calculations. Our semicore PP sX-LDA band gaps agree well with the experimental ones, and the sX-LDA d state energy levels agree better with experiment than the GW results. Our semicore PP sX-LDA results also agree well with the FLAPW sX-LDA results.

We point out that the inclusion of semicore states makes computations more expensive than the conventional PP calculations due to a large plane wave cutoff energy. Typically,

the cutoff energy required for a semicore PP calculation is about three times larger than the cutoff energy needed for a PP calculation without semicore states. Although the semicore PP enables one to calculate sX-LDA with plane wave basis, it is more desirable to use the original plane wave cutoff energy. The knowledge obtained in our current study provide us with insights for how to correct the d-s, d-p, and d-d screened-exchange integrals without including the semicore states. This ongoing study will be reported in the future.[28]

This work was supported by the DMS/BES/SC, and MICS/SC offices of the U.S. Department of Energy under Contract No. DE-AC02-05CH11231. It used the resources of National Energy Research Scientific Computing Center (NERSC).

[1] P. Hohenberg and W. Kohn, Phys. Rev. **136**, B864 (1964).

[2] W. Kohn and L. J. Sham, Phys. Rev. **140**, A1133 (1965).

[3] J. C. Phillips, Phys. Rev. **112**, 685 (1958).

[4] M. L. Cohen and V. Heine, in *Solid State Physics, Advances in Research and Application*, edited by F. Seitz, D. Turnbull, and H. Ehrenreich (Academic, New York, 1970), Vol. 24, p. 37.

[5] M. T. Yin and M. L. Cohen, Phys. Rev. B **25**, 7403 (1982).

[6] D. M. Bylander and L. Kleinman, Phys. Rev. B **41**, 7868 (1990).

[7] A. Seidl, A. Gorling, P. Vogl, J. A. Majewski, and M. Levy, Phys. Rev. B **53**, 3764 (1996).

[8] C. B. Geller, W. Wolf, S. Picozzi, A. Continenza, R. Asahi, W. Mannstadt, A. J. Freeman, and E. Wimmer, Appl. Phys. Lett. **79**, 368 (2001).

[9] D. Vogel, P. Krüger, and J. Pollmann, Phys. Rev. B **54**, 5495 (1996).

[10] D. Vogel, P. Krüger, and J. Pollmann, Phys. Rev. B **55**, 12836 (1997).

[11] A. Filippetti, and N. A. Spaldin, Phys. Rev. B **67**, 125109 (2003).

[12] B. Lee, L.-W. Wang, C. D. Spataru, and S. G. Louie, Phys. Rev. B **76**, 245114 (2007).

[13] M. Moukara, M. Städele, J. A. Majewski, P. Vogl, and A.Görling, J. Phys. Conds. Matter **12**, 6783 (2000).

[14] F. R. Vukajlovic, E. L. Shirley, and R. M. Martin, Phys. Rev. B **43**, 3994 (1991).

[15] J. R. Trail and R. J. Needs, J. Chem. Phys. **122**, 014112 (2005).

[16] E. Engel, A. Höck, R. N. Schmid, R. M. Dreizler, and N. Chetty, Phys. Rev. B **64**, 125111 (2001).

[17] M. Rohlfing, P. Krüger, and J. Pollmann, Phys. Rev. B **57**, 6485 (1998).

[18] W. Luo, S. Ismail-Beigi, M. L. Cohen, and S. G. Louie, Phys. Rev. B **66**, 195215 (2002).

[19] K. Lawniczak-Jablonska, T. Suski, I. Gorczyca, N. E. Christensen, K. E. Attenkofer, E. M. G. R. C. C. Perera, J. H. Underwood, D. L. Ederer, and Z. L. Weber, Phys. Rev. B **61**, 16623 (2000).

[20] J. Wu, W. Walukiewicz, K. M. Yu, J. W. A. III, E. E. Haller, H. Lu, J. Schaff, Y. Saito, and Y. Nanishi, Appl. Phys. Lett. **80**, 3967 (2002).

[21] A. Fleszar and W. Hanke, Phys. Rev. B **71**, 045207 (2005).

[22] R. Weidemann, H.-E. Gumlich, M. Kupsch, and H.-U. Middelmann, Phys. Rev. B **45**, 1172 (1992).

[23] L. Ley, R. A. Pollak, F. R. McFeely, S. P. Kowalczyk, and D. A. Shirley, Phys. Rev. B **9**, 600 (1974).

[24] O. Madelung, M. Schulz, and H. Weiss, eds., *Intrinsic Properties of Group IV Elements and III-V, II-VI, and I-VII Compounds*, vol. 22 Pt. a of *Landolt-Bornstein, New Series* (Springer, Berlin, 1987).

[25] A. P. J. Stampfl, P. Hofmann, O. Schaff, and A. M. Bradshaw, Phys. Rev. B **55**, 9679 (1997).

[26] D. R. T. Zahn, G. Kudlek, U. Rossow, A. Hoffmann, I. Broser, and W. Richter, Adv. Mater. Opt. Electron. **3**, 11 (1994).

[27] S. A. Ding, G. Neuhold, J. H. Weaver, P. Häberle, K. Horn, O. Brandt, H. Yang, and K. Ploog, J. Vac. Sci. Technol. A **14**, 819 (1996).

[28] B. Lee and L.-W. Wang, (in preparation).

TABLE I: Comparison of different pseudopotentials. ϵ_l^{PP}, and ϵ_l^{AE} are the LDA results of highest occupied atomic eigenvalue with l angular momentum from (+20/+21) pseudopotential and all-electron calculations, respectively. $K_{ll'}(+12/+13)$, $K_{ll'}(+20/+21)$), and $K_{ll'}(AE)$ are the screened-exchange integrals evaluated using $\phi_l(r)$, from (+12/+13) pseudopotential, (+20/+21) pseudopotential, and all-electron wavefunctions, respectively. We used the same screening length as in the test bulk calculations; ZnS, CdS, and InN valence electron average densities were used for k_{TF} in Zn, Cd, and In atoms, respectively. We averaged the screened-exchange integral for an angular momentum over the magnetic quantum numbers.

	Zn	Cd	In
$\epsilon_s^{PP} - \epsilon_s^{AE}$ (eV)	-0.034	-0.052	-0.073
$\epsilon_p^{PP} - \epsilon_p^{AE}$ (eV)			0.007
$\epsilon_d^{PP} - \epsilon_d^{AE}$ (eV)	0.089	0.112	0.163
$K_{ss}(+12/+13)/K_{ss}(AE)$	1.04	1.11	1.10
$K_{ss}(+20/+21)/K_{ss}(AE)$	1.05	1.13	1.13
$K_{sp}(+12/+13)/K_{sp}(AE)$	1.02	1.05	1.05
$K_{sp}(+20/+21)/K_{sp}(AE)$	1.01	1.03	1.03
$K_{sd}(+12/+13)/K_{sd}(AE)$	2.38	1.85	2.10
$K_{sd}(+20/+21)/K_{sd}(AE)$	1.15	1.24	1.24
$K_{pp}(+12/+13)/K_{pp}(AE)$	1.01	1.02	1.02
$K_{pp}(+20/+21)/K_{pp}(AE)$	1.00	1.02	1.01
$K_{pd}(+12/+13)/K_{pd}(AE)$	1.99	1.60	1.72
$K_{pd}(+20/+21)/K_{pd}(AE)$	1.10	1.13	1.12
$K_{dd}(+12/+13)/K_{dd}(AE)$	0.62	0.94	0.90
$K_{dd}(+20/+21)/K_{dd}(AE)$	0.99	0.99	0.99

TABLE II: The band gap energy (E_g) and the semicore d state binding energy (E_d) in eV. All systems were calculated for the zinc-blende structure using experimental lattice constants (and k_F corresponding to average charge density); 5.67 (2.57), 5.41 (2.69), 5.82 (2.50), and 4.98 (2.92) Å(Å^{-1}) for ZnSe, ZnS, CdS, and InN, respectively. The d state binding energy is defined as the eigenvalue difference between the top most valence band state energy and the highest d state energy at Γ point. PP and AE denote pseudopotential and FLAPW calculations, respectively. For PP LDA and PP sX-LDA results, the numbers outside and inside the parenthesis are the results using (+20/+21) PP's and (+12/+13) PP's, respectively, For comparability reason, we list plane wave LDA based GW calculation results with a random-phase approximation for the screened Coulomb interaction and a plasmon-pole model for the dynamics of the screening. In all these calculations, the spin-orbit effects were not taken into account.

		ZnSe	ZnS	CdS	InN
PP LDA	E_g	0.94 (0.97)	1.66 (1.70)	0.84 (0.84)	-0.38 (-0.42)
	E_d	-6.21 (-6.61)	-5.91 (-6.22)	-7.17 (-7.46)	-12.79 (-13.31)
PP sX-LDA	E_g	2.42 (1.41)	3.24 (2.41)	2.06 (1.78)	0.39 (0.08)
	E_d	-9.59 (-9.32)	-8.83 (-8.64)	-8.71 (-9.23)	-14.61 (-15.26)
AE LDA	E_g	0.98	1.81	0.82	-0.47
AE sX-LDA	E_g	2.57[a]	3.67[a]	2.37[a]	
GW	E_g	2.32[b], 2.24[d]	3.19[b], 3.50[d], 3.38[c]	2.45[d], 2.11[c]	
	E_d	-7.0[b], -7.31[c]	-6.9[b], -6.4[d], 6.87[c]	-8.1[d], -7.55[c]	
Experiment	E_g	2.82[e]	3.78[e]	2.48[f]	0.8[h]
	E_d	-9.37[i], -9.20[j]	-9.0[e]	-9.2[k]	

[a]Reference 8.

[b]Reference 18.

[c]Reference 21.

[d]Reference 17.

[e]Reference 24.

[f]Reference 26.

[g]Reference 19.

[h]Reference 20.

[i]Reference 22.

[j]Reference 23.

[k]Reference 25.

[l]Reference 27.

TABLE III: Comparison of difference Zn pseudopotential results for ZnS.

	Zn^{+12}, r_c^d=3.0 a_0	Zn^{+12}, r_c^d=1.0 a_0	Zn^{+20}, r_c^d=0.9 a_0
K_{sd}(PP)/K_{sd}(AE)	2.38	1.42	1.15
K_{pd}(PP)/K_{pd}(AE)	1.99	1.22	1.10
K_{dd}(PP)/K_{dd}(AE)	0.62	0.99	0.99
E_g^{LDA} (eV)	1.70	1.79	1.66
$E_g^{\text{sX-LDA}}$ (eV)	2.41	3.20	3.24
E_d^{LDA} (eV)	-6.22	-6.12	-5.91
$E_d^{\text{sX-LDA}}$ (eV)	-8.64	-9.92	-8.83
E_{cut} (Ry)	80	200	250

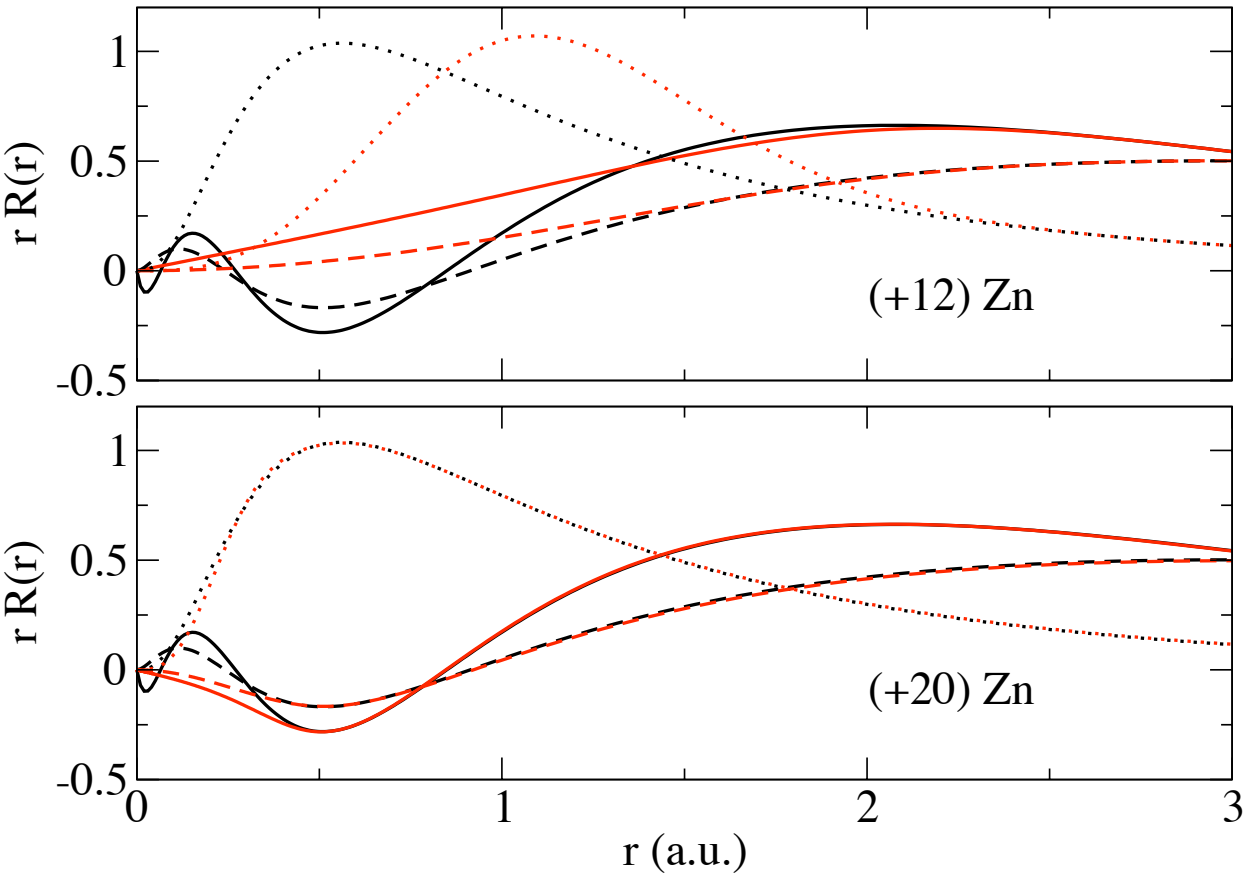

FIG. 1: Radial wavefunctions, $u(r) = rR(r)$, of Zn atom calculated in LDA. Upper panel: All-electron wavefunctions (black lines) and (+12) Zn pseudopotential wavefunctions (red lines) are shown. Solid, dashed, and dotted lines are for s, p, and d angular momentum, respectively. Lower panel: Same as the upper panel except that (+20) Zn pseudopotential is used instead of (+12) Zn.

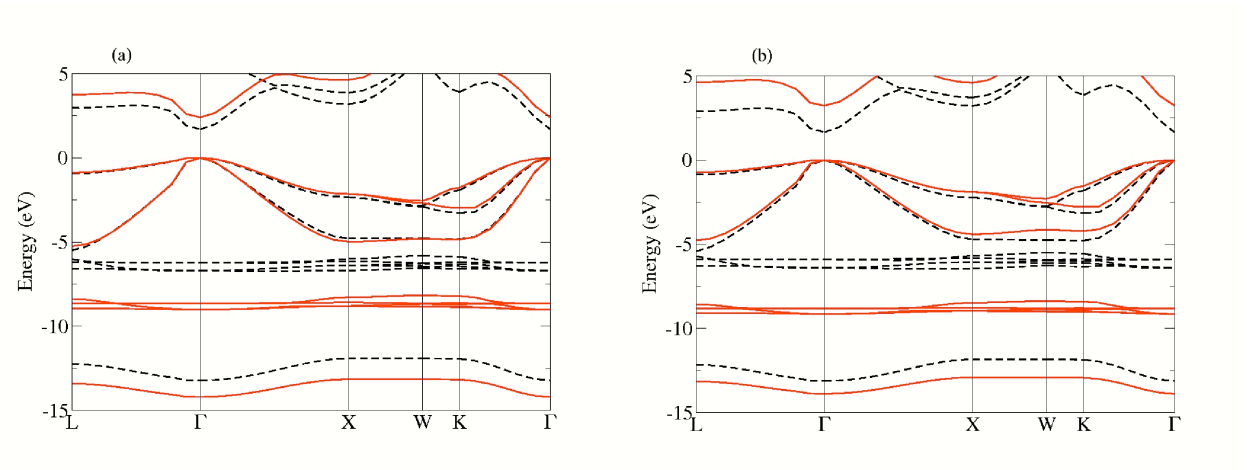

FIG. 2: Band structure of zinc-blende ZnS. The dashed and solid lines denote the electron bands calculated from LDA and sX-LDA, respectively. (a) Zn^{+12} core is used for the Zn pseudopotential. (b) Zn^{+20} core is used for the Zn pseudopotential. LDA and sX-LDA bands are shifted so that the valence band maximum be placed at zero energy.

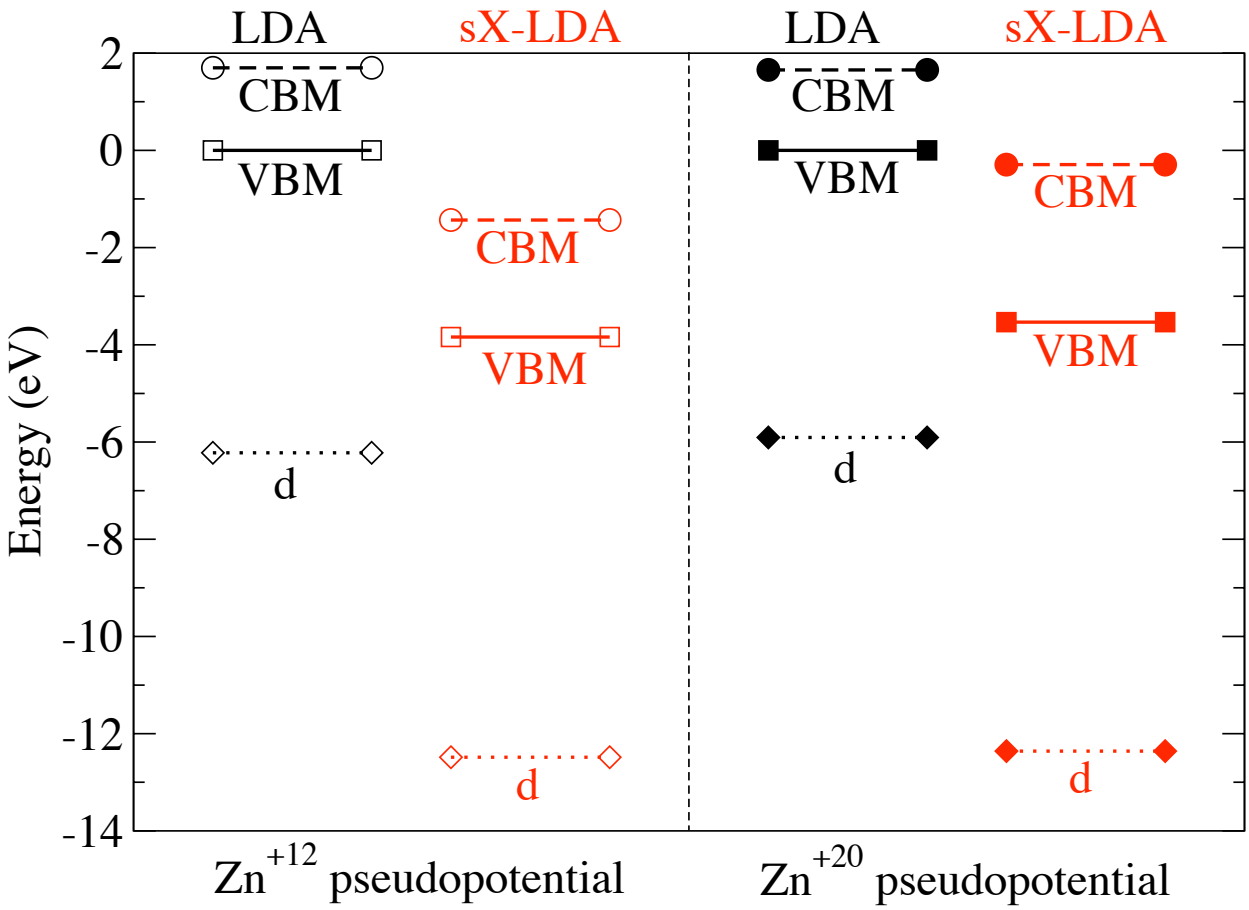

FIG. 3: Comparision of zinc-blende ZnS band edge states in LDA and sX-LDA method. The dashed, solid, and dotted lines denote the electron energy at CBM, VBM, and top d band state in order. Black and red lines correspond to LDA and sX-LDA, respectively. LDA and sX-LDA bands are shifted relative to the LDA VBM energy. The comparison of absolute eigenvalues in different methods is made for each pseudopotential. For each pseudopotential, i.e., Zn^{+12} PP and Zn^{+20} PP separately, the downshift of sX-LDA eigenvalues is seen. The plot also shows that the lowering of VBM eigenenergy is larger than CBM eigenvalue downshift.